Latin American Journal of Solids and Structures
www.lajss.org

Design Optimization of a Random Suspension Device Considering a Reliability Constraint on the Frequency Response Function

Abstract

This work deals with the design of a suspension device, idealized as a spring-mass-damper system. The amplitude of a nominal system is constrained to satisfy certain limitations in a given frequency band and the design is to be done as a reliability-based optimization. This constitutes a major difficulty since the constraint becomes a random process. To concentrate in the main ideas, only the stiffness of the system will be considered random. The stiffness is characterized by a uniform random variable, and its mean and standard deviation are the optimization parameters. The design problem is stated as a two-objective optimization. They are the mean and the standard deviation of the stiffness: one search for the lowest stiffness and the greatest standard deviation, while the amplitude response must be within the acceptable domain of vibration, which is prescribed. To generate the Pareto front, the Normal Boundary Intersection method is used in the RFNM algorithm. Results show that a not-connected Pareto curve can be obtained for some choice of constraint. Hence, in this simple example, one shows that difficult situations can occur in the design of dynamic systems when prescribing an amplitude-response hull. Despite the simplicity of the example treated here, chosen to highlight the main ideas without distraction, the strategy proposed here can be generalized for more complex cases and give valuable results, able to help designers to choose for the best compromise between the mean and the standard deviation in reliability-based designs.

Keywords

Structural dynamic, random system, uncertainty, multi-objective optimization, Pareto front.

Emmanuel Pagnacco [a]
Hafid Zidani [b]
Rubens Sampaio [c]
Eduardo Souza de Cursi [d]
Rachid Ellaia [e]

[a] LOFiMS, EA 3828, INSA de Rouen, BP 8, 76801 Saint-Etienne du Rouvray, France
Emmanuel.Pagnacco@insa-rouen.fr
[b] LERMA, Mohammed V University in Rabat, Mohammadia School of Engineers, Rabat, BP 765, Ibn Sina avenue, Agdal, Morocco
hafidzidani@yahoo.fr
[c] PUC-Rio, Mechanical Eng. Dept., Rua Marquês de São Vicente, 225; 22453-900 Rio de Janeiro RJ. Brazil
rsampaio@puc-rio.br
[d] LOFiMS, EA 3828, INSA de Rouen, BP 8, 76801 Saint-Etienne du Rouvray, France
souza@insa-rouen.fr
[e] LERMA, Mohammed V University in Rabat, Mohammadia School of Engineers, Rabat, BP 765, Ibn Sina avenue, Agdal, Morocco
ellaia@emi.ac.ma

http://dx.doi.org/10.1590/1679-78252151

Received 19.05.2015
In revised form 04.02.2016
Accepted 12.02.2016
Available online 27.02.2016

1 INTRODUCTION

In this study, the reliable design of a suspension device is considered. It is idealized as a spring-mass-damper, having linear behavior, leading to a simple single-degree-of-freedom (SDOF) dynamic system. The design parameter of interest is chosen to be the spring stiffness, while the design constraint consists in the prescription of a curve giving the acceptable amplitude response hull for the system responses over a given frequency range. That is, in the given frequency range the frequency response function (FRF) of the system, for any value of the stiffness, must be within the prescribed region. Considering this constraint for a random system leads to a difficult situation that involves a stochastic process having the frequency as parameter for the reliability-based design optimization. We propose in this work to replace this difficult problem by a simpler one, resulting from a discretization procedure. In our approach, a vector replaces the constraint process where each of his components is obtained for a fixed value of the frequency. We will see with the application treated in this work that this leads to an acceptable numerical solution from an engineer point of view.

In order to focus on the main ideas, only the stiffness of the system is chosen to be uncertain in the system. More precisely, we chose to study the specific case of a bounded distribution for the stiffness, which leads us to consider a uniform distribution, which is a consequence of the Maximum Entropy Principle. Then, the stiffness can be characterized by its mean and standard deviation, which become the design parameters. Moreover, since the design is a reliability-based optimization, one has to think now in terms of probability of acceptance for the design constraint. Thus, the acceptable reliability, specified by the designer, is an additional parameter of the problem.

To distinguish among the numerous design solutions, a vector objective function has to be defined, which leads to formulate an optimization problem in its standard form. Two scalar objective functions are chosen. One searches a suspension having the lowest mean stiffness, in order to keep low the cost of material, and the greatest standard deviation, in order to keep low the manufacturing costs. So the mean and the standard deviation of the random stiffness are the design objectives.

Let us described how the present study is organized: in the Section 2, generalities of interest about the mechanical design are presented, when considering the reliability of the structures. The Section 3 gives the equations of vibration to consider for the SDOF system and the adopted stochastic formulation. The Section 4 describes the choice of objective functions, the reliability constraints, a general way to evaluate them, and gives the resulting formulation for the multi-objective reliability based optimization problem. The Section 5 gives important results for the uncertainty propagation, which helps to link the reliability to the system random parameter. The Section 6 describes the Normal Boundary Intersection (NBI) method that is used to generate the Pareto front and the RFNM optimization algorithm (for Representation Formula Nelder-Mead). Finally, the last Section 7 describes the results of the application, where unusual Pareto front are found, and the mechanical interpretation of the design for this vibration problem is thoroughly discussed.

2 DESIGNING FOR STRUCTURAL RELIABILITY

When a structure is loaded it deforms and develops internal stresses. This deformation and internal stresses must be within certain bounds which characterize the resistance of the material. That is, within the bounds the integrity and proper function of the structure are assured. Outside the bounds

one says that the structure fails. The boundary between these two situations is known as the limit-state.

A simple example of ultimate limit-state is the Von Mises stress s compared to an acceptable resistance r of the structural material. Examples of serviceability limit-state can be a maximum deflection or an excessive vibration which do not exceed a human comfort threshold. Then, considering a continuous structure it is required to analyze not only one spatial point of it but all points to ensure its design. To use standard Probability Theory, leads us to define a vector of limit states when adopting a spatial numerical description associated to a mesh of the mechanical part for a field.

Thus, the engineering task consists generally in finding the nominal design described by the set of parameters $\mathbf{x} \in \mathbb{R}^n$ which optimize an objective vector function $\mathbf{f} : \mathbb{R}^n \to \mathbb{R}^q$, subject to a vector failure criteria $\mathbf{g} : \mathbb{R}^n \to \mathbb{R}^g$. A typical formulation reads:

$$\begin{aligned} &\min_{\mathbf{x}} \left(\mathbf{f}\left(\mathbf{x}\right)\right) \\ &\mathbf{g}\left(\mathbf{x}\right) = \mathbf{r}\left(\mathbf{x}\right) - \mathbf{s}\left(\mathbf{x}\right) > \mathbf{0} \end{aligned} \tag{1}$$

where $\mathbf{s}$ is the load and $\mathbf{r}$ is the resistance, g denotes the number of control (spatial) points over the structure. However, the design solution which satisfies this formulation does not take into account uncertainties, which implies the possibility of undesirable structural responses in presence of them. Thus, to handle structural or loading uncertainties it is preferable to think in terms of reliability when introducing a stochastic framework (Choi et al. 2007, Lemaire 2009, Souza de Cursi and Sampaio 2015). In the sequel, the random variables are distinguished from the deterministic ones by denoting them in capital letters. Then, to deal with the uncertainties, we introduce an additional set of random processes $\mathbf{Y}$ which has to be considered in the structural design, and the structure will be considered unreliable if the failure probability of the limit-state exceeds a prescribed value. Limit-state functions $\mathbf{G}$ and probability of failure $\mathbf{P}_f$ are defined as:

$$\begin{aligned} &\mathbf{G}\left(\mathbf{x}, \mathbf{Y}\right) = \mathbf{R}(\mathbf{x}, \mathbf{Y}) - \mathbf{S}(\mathbf{x}, \mathbf{Y}) \\ &\mathbf{P}_{\mathrm{f}} = \mathrm{Prob}\left[\mathbf{G}\left(\mathbf{x}, \mathbf{Y}\right) < \mathbf{0}\right] \end{aligned} \tag{2}$$

Both $\mathbf{R}$ and $\mathbf{S}$ are now functions of the nominal design variable $\mathbf{x}$ and the random processes $\mathbf{Y}$. The probability space to be used is $(\Omega, \mathcal{A}, P)$, where Ω is the set of sample space, $\mathcal{A}$ is an event space of subsets of Ω and P is a probability measure on $(\Omega, \mathcal{A})$.

The failure region is delimitated by $\mathbf{G} < \mathbf{0}$ while $\mathbf{G} = \mathbf{0}$ and $\mathbf{G} > \mathbf{0}$ indicate the limit state and the safe region, respectively. Note that the non-failure probability $\mathbf{P}_{\mathrm{r}}$ is:

$$\mathbf{P}_{\mathrm{r}} = 1 - \mathbf{P}_{\mathrm{f}} \tag{3}$$

In the reliability problem it is also prescribed an admissible reliability, $\overline{\mathbf{P}}_{\mathrm{r}}$.

3 FORMULATION OF THE STOCHASTIC VIBRATION PROBLEM

3.1 Equations for the Vibration Problem

Vibrations can often lead to undesirable results, such as discomfort or fatigue of passengers of a car whose suspension was not properly designed. Structural and mechanical failure can often result from sustained vibration. In this study, we are interesting in designing the stiffness of a mechanical device. To limit vibration risk, specifications are set for the amount of vibration a device can withstand. Hence, in designing, it is of interest to adjust the physical parameters of the system in such a way that the vibration response meets the specified peak level given by the specification. Generally, a hull of acceptable peaks levels of vibration are established in the frequency domain and are express in terms of accelerations, but it can be express also in peaks displacements without difficulty.

To fix ideas, we can consider the most simple case of a device which is idealized as a simple linear spring-damper-mass system fixed at one end and subjected to an imposed harmonic displacement z at the other end (sketched in Figure 1). In the frequency domain, the displacement of this single degree of freedom (SDOF) system, u, is given by Lin (1967):

$$\left(k - m\left(2\pi f\right)^2 + \mathrm{j}\ 2\pi f c\right) u\left(f\right) = r\left(f\right) \tag{4}$$

$$\text{with:} \qquad r\left(f\right) = m\left(2\pi f\right)^2 z\left(f\right) \tag{5}$$

where f is the frequency. In this equation, k, m and c are the stiffness, mass and damping system parameters (respectively), and the displacement $u\left(f\right)$ is obtained by solving equation (4), leading to:

$$u\left(f\right) = \frac{r\left(f\right)}{k - m\left(2\pi f\right)^2 + \mathrm{j}\ 2\pi f c} \tag{6}$$

In contrast to a general mechanical problem which is continuous in the space dimension, this simple system has only one spatial degree of freedom.

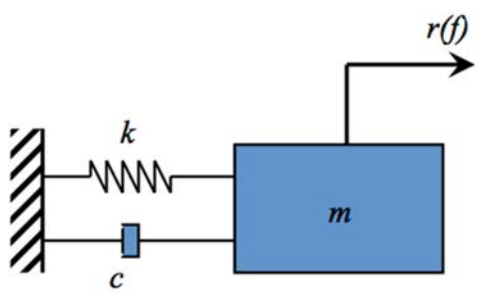

Figure 1: SDOF system.

To study this system, it is of interest to introduce the FRF $h\left(f\right)$ given by a unit forcing, leading to:

$$h(f) = \frac{1}{k - m(2\pi f)^2 + \mathrm{j}\ 2\pi fc} \tag{7}$$

which has the amplitude:

$$|h(f)| = \frac{1}{\sqrt{\left(k - m(2\pi f)^2\right)^2 + (2\pi fc)^2}} \tag{8}$$

Hence, amplitude of the Frequency Response Function depends non-linearly of the stiffness of the component.

More generally, frequency response function of a discrete system obtain by a finite element analysis or frequency response function of a continuous system could also be considered in this study.

3.2 Stochastic Formulation of the Mechanical Problem

The mechanical system becomes stochastic when stiffness parameters or the loads (or both) are no longer deterministic. In the sequel, random variables will be denoted capitalizing the letter that represents the deterministic variable, hence K and U in this case for the stiffness and the response amplitude.

The formulation adopted in this study is based on peak amplitudes of the system response. Considering the SDOF device has a random stiffness, the amplitude system response is a random process, which leads to study:

$$U_K(f) = \frac{1}{\sqrt{\left(K - m(2\pi f)^2\right)^2 + (2\pi fc)^2}} \tag{9}$$

for a unit forcing function.

In this study, the probability law for the random variable K is chosen from the Maximum Entropy Principle (Kapur and Kesavan 1992, Rubinstein and Kroese 2008). This principle states that the uniform probability maximizes the entropy in the case of bounded domain of the random variable. Thus, the probability density function (PDF) given by the constant value $p_K(k) = \frac{1}{2\sqrt{3}\sigma_K}$ over $[\mu_K - \sqrt{3}\sigma_K, \mu_K + \sqrt{3}\sigma_K]$ is adopted for the random variable K, where μ_K denotes its mean value and σ_K its standard deviation. From the problem description proposed in the previous section, the set of random processes is $\mathbf{Y} = \{K; U(f)\}$ and the vector of design parameters is $\mathbf{x} = \{\mu_K, \sigma_K\}$. Note in such a case that μ_K has to be greater than $\sqrt{3}\sigma_K$ to ensure a positive stiffness while σ_K has to be non-negative.

4 FORMULATION OF THE RELIABILITY-BASED DESIGN OPTIMIZATION PROBLEM

4.1 Objective Functions

From a design point of view, an interesting objective is to design springs with the lowest stiffness in order to generate significant economical gains due to cheaper material. But another economical interesting point is to authorize a large dispersion about the nominal design when building multiple springs, that is do not be strict about the manufacture. Thus, the optimization problem of interest is posed such as the one which minimize the mean stiffness μ_K and which simultaneously maximize its standard deviation σ_K, to reduce manufacture costs. This leads to a two-objective optimization problem ($q = 2$).

4.2 Reliability Constraints

From a design point of view, the amplitude of the vibration response has to respect the bound for the peak level given by the specification, at least within a chosen reliability value $\overline{P}_r$. This define the limit state as:

$$\mathsf{G}\left(\mathbf{x}, \mathbf{Y}\right) = u_{\max}\left(f\right) - U_K\left(f\right) \qquad \text{for } f \in \mathcal{B} \tag{10}$$

where $u_{\max} : \mathcal{B} \to \mathbb{R}$ denotes the bound for the peak amplitude limit given by the specification and $\mathcal{B} = \left[0, f_{\max}\right]$. To focus on main ideas in our problem, the peak limit function $u_{\max}\left(f\right)$ is considered deterministic. Thus, we can write the non-failure probability as:

$$\text{Prob}\left[U_K\left(f\right) \leq u_{\max}\left(f\right)\right] = P_U\left(u_{\max}; f\right) \tag{11}$$

where P_U denotes the cumulative distribution function of the system amplitude response U_K at the fixed frequency f, thus:

$$\text{Prob}\left[U_K\left(f\right) \leq u_{\max}\left(f\right)\right] = \int_0^{u_{\max}(f)} p_U\left(u; f\right)\mathrm{d}u = \int_{u_{\inf}(f)}^{u_{\max}(f)} p_U\left(u; f\right)\mathrm{d}u \tag{12}$$

$p_U\left(u; f\right)$ being the probability density function (PDF) of the system and $u_{\inf}\left(f\right) = \inf\left\{u : p_U\left(u; f\right) > 0\right\}$ is the left endpoint of the support of P_U.

For a general problem, the distribution function of the system response amplitude is linked to the system random variables. Hence, considering a set $\mathbf{Z}$ of random variables and the system response function $U_{\mathbf{Z}}$, we have:

$$P_U\left(u; f\right) = \int \ldots \int_{U_{\mathbf{Z}}(f) \leq u} p_{\mathbf{Z}}\left(\mathbf{z}\right)\mathrm{d}\mathbf{z} \tag{13}$$

where $p_{\mathbf{Z}}\left(\mathbf{z}\right)$ is the joint PDF of variables $\mathbf{Z}$. Evaluating this expression is generally not straightforward. It is necessary to use a numerical method, such as, for example, the Monte Carlo simulation

method. In addition, to handle the continuous limit state linked to the random processes set, it is sampled at e fixed frequencies, leading to:

$$\mathrm{P}_{U_j} = \mathrm{Prob}\left[U_K\left(f_j\right) \le u_{\max}\left(f_j\right)\right] \qquad \text{for } j \in \left[1,\ldots,e\right] \tag{14}$$

which are collected in the vector $\mathbf{P}_U$ of probabilities.

A possible general way to evaluate numerically this probabilities vector is the Monte Carlo numerical simulation method:

1. Choose $\mathbf{x} = \left\{\mu_K,\ \sigma_K\right\}$, $\mathcal{B} = \left[0,\ f_{\max}\right]$, and $u_{\max} : \mathcal{B} \to \mathbb{R}$;
2. Generate an event $K\left(\omega\right)$;
3. For a sampling set of $\mathcal{B}$, $\mathcal{B}_e$, composed from e components, compute for each frequency $f \in \mathcal{B}_e$:
   a) $U_K\left(\omega, f\right)$; that is, compute the displacement amplitude for the $K\left(\omega\right)$ generated at step 2 by solving the vibration problem at the frequency f;
   b) Evaluate the component $P_{U_j}\left(u_{\max}; f\right)$ of the $\mathbb{R}^e$ vector $\mathbf{P}_U$ related to the considered frequency f from the Monte Carlo simulation method; that is compute the ratio between the number of displacement amplitude that are lower than the peak limit function $u_{\max}\left(f\right)$ and the total number of the element of the event;

4.3 Resulting Formulation

Consequently, the reliability based design optimization problem has the following multi-objective form:

$$\begin{cases} \min\ \mathcal{F}\left(\mathbf{x}\right) = & \left[\mu_K, -\sigma_K\right]^{\mathrm{T}} \\ \text{subject to:} & \mathrm{Prob}\left[U_K\left(f_j\right) < u_{\max}\left(f_j\right)\right] \ge \overline{P}_{\mathrm{r}}, \quad \text{for } j = 1,\ldots,e \\ & \mu_K > \sqrt{3}\sigma_K,\ \sigma_K \ge 0 \\ & K \sim \mathrm{Uniform}\left(\mathbf{x}\right) \end{cases} \tag{15}$$

with the two-parameter vector $\mathbf{x} = \begin{bmatrix} \mu_K \\ \sigma_K \end{bmatrix}$ $(n = 2)$.

Multi-objective optimization involves the simultaneous optimization of several incommensurable and often competing objectives. Since there is no preference information, a non-dominated set of solutions is obtained, instead of a single optimal solution. These optimal solutions are termed as Pareto optimal solutions. Stated in another way, Pareto optimal points are the solutions of the optimization which cannot be improved in one objective function without deteriorating their performance in at least one of the other objectives. Hence, for a multi-objective problem the solution of the problem can be viewed as the Pareto front.

5 UNCERTAINTIES PROPAGATION RESULT FOR THE SDOF SYSTEM HAVING A STIFFNESS WHICH FOLLOWS A UNIFORM DISTRIBUTION

For an SDOF problem, there is only one single random variable K in the set $\mathbf{Z}$, and an analytical expression can be derived instead of using a Monte Carlo numerical simulation method. By using $p_U(u) = \frac{\mathrm{d}P_u}{\mathrm{d}u}$, it is found that (Zwillinger and Kokoska, 2000):

$$p_U(u) = \frac{1}{\left|\frac{\mathrm{d}U}{\mathrm{d}K}\right|_{k_1}} p_K(k_1) + \cdots + \frac{1}{\left|\frac{\mathrm{d}U}{\mathrm{d}K}\right|_{k_p}} p_K(k_p) \tag{16}$$

In this expression, k_j for $j = 1,\ldots,p$ denotes the roots of the algebraic equation $u(k,f) = u$, for f fixed (notice that $j = 1$ for a bijective function). By considering a uniform distribution for the stiffness random variable such that:

$$p_K(k) = p_K = \frac{1}{2\sqrt{3}\sigma_K} \tag{17}$$

having the mean μ_K, this produces (Pagnacco et al. 2015):

$$p_U(u,f) = \begin{cases} \dfrac{1}{u^2\sqrt{1-\left(2\pi f c u\right)^2}} \times p_K & \text{if} \quad u_{\inf}(f) \le u(f) \le u_1(f) \\ \dfrac{2}{u^2\sqrt{1-\left(2\pi f c u\right)^2}} \times p_K & \text{if} \quad u_1(f) \le u(f) \le u_{\sup}(f) \\ 0 & \text{elsewhere} \end{cases} \tag{18}$$

where:

- $u_{\sup}(f)$ denotes the upper envelope of the system response which is given by:

$$u_{\sup}(f) = \begin{cases} \dfrac{1}{\sqrt{\left(k_{\inf} - m\left(2\pi f\right)^2\right)^2 + 4\pi^2 c^2 f^2}} & \text{for } \left(2\pi f\right)^2 \in \left[0, \dfrac{k_{\inf}}{m}\right] \\ \dfrac{1}{2\pi f c} & \text{for } \left(2\pi f\right)^2 \in \left[\dfrac{k_{\inf}}{m}, \dfrac{k_{\sup}}{m}\right] \\ \dfrac{1}{\sqrt{\left(k_{\sup} - m\left(2\pi f\right)^2\right)^2 + 4\pi^2 c^2 f^2}} & \text{for } \left(2\pi f\right)^2 \in \left[\dfrac{k_{\sup}}{m}, +\infty\right[\end{cases} \tag{19}$$

- $u_{\inf}(f)$ denotes the lower envelope of the system response given by:

$$u_{\inf}\left(f\right)=\begin{cases}\dfrac{1}{\sqrt{\left(k_{\inf}-m\left(2\pi f\right)^2\right)^2+4\pi^2c^2f^2}} & \text{for } \left(2\pi f\right)^2\in\left[0,\mu_K\right]\\ \dfrac{1}{\sqrt{\left(k_{\sup}-m\left(2\pi f\right)^2\right)^2+4\pi^2c^2f^2}} & \text{for } \left(2\pi f\right)^2\in\left[\mu_K,+\infty\right[\end{cases} \tag{20}$$

- $u_1\left(f\right)$ denotes the domain where there is two roots. It is given by:

$$u_1\left(f\right)=\begin{cases}\dfrac{1}{\sqrt{\left(k_{\inf}-m\left(2\pi f\right)^2\right)^2+4\pi^2c^2f^2}} & \text{for } \left(2\pi f\right)^2\in\left[\dfrac{k_{\inf}}{m},\mu_K\right]\\ \dfrac{1}{\sqrt{\left(k_{\sup}-m\left(2\pi f\right)^2\right)^2+4\pi^2c^2f^2}} & \text{for } \left(2\pi f\right)^2\in\left[\mu_K,\dfrac{k_{\sup}}{m}\right[\end{cases} \tag{21}$$

and we defined $u_1\left(f\right)=u_{\sup}\left(f\right)$ elsewhere for convenience.

Then, it is possible to evaluate $\mathrm{P}_U\left(f\right)$ the reliability for a fixed frequency by integrating the PDF given by Equation 18 which leads to:

$$\mathrm{P}_U\left(f\right)=\mathrm{Prob}\left[u_{\max}\left(f\right)-U_K\left(f\right)<0\right]=\int_{u_{\inf}}^{u_{\max}}p_U\left(u,f\right)\mathrm{d}u \tag{22}$$

such that:

$$\mathrm{P}_U\left(f\right)=\begin{cases}0 & \text{if } u_{\max}\left(f\right)<u_{\inf}\left(f\right)\\ \dfrac{p_K}{u_{\inf}}\sqrt{1-\varsigma^2u_{\inf}^2}-\dfrac{p_K}{u_{\max}}\sqrt{1-\varsigma^2u_{\max}^2} & \text{if } u_{\inf}\left(f\right)\le u_{\max}\left(f\right)<u_1\left(f\right)\\ \dfrac{p_K}{u_{\inf}}\sqrt{1-\varsigma^2u_{\inf}^2}+\dfrac{p_K}{u_1}\sqrt{1-\varsigma^2u_1^2}-\dfrac{2p_K}{u_{\max}}\sqrt{1-\varsigma^2u_{\max}^2} & \text{if } u_1\left(f\right)\le u_{\max}\left(f\right)<u_{\sup}\left(f\right)\\ 1 & \text{if } u_{\max}\left(f\right)>u_{\sup}\left(f\right)\end{cases} \tag{23}$$

where $\varsigma=2\pi fc$. Moreover, it is also possible to invert the integral of the PDF with an unknown upper boundary u_{p} to find the iso-quantile function:

$$\int_{u_{\inf}}^{u_{\mathrm{p}}}p_U\left(u,f\right)\mathrm{d}u=\overline{P}_{\mathrm{r}} \tag{24}$$

which leads to:

$$u_{\mathrm{p}}\left(f\right)=\begin{cases}u_{\mathrm{P}_2}\left(f\right) & \text{if } u_{\mathrm{P}_1}\left(f\right)>u_1\left(f\right)\\ u_{\mathrm{P}_1}\left(f\right) & \text{elsewhere}\end{cases} \tag{25}$$

with:

$$u_{\mathrm{P}_1}(f) = \frac{p_K}{\sqrt{\varsigma^2 \mu_K p_K^2 + \left(\overline{P}_{\mathrm{r}} - p_K \sqrt{\frac{1}{u_{\mathrm{inf}}^2} - \varsigma^2} \right)^2}} \tag{26}$$

and:

$$u_{\mathrm{P}_2}(f) = \frac{p_K}{\sqrt{\varsigma^2 \mu_K p_K^2 + \left(\overline{P}_{\mathrm{r}} - p_K \sqrt{\frac{1}{u_{\mathrm{inf}}^2} - \varsigma^2} - \frac{1}{2} p_K \sqrt{\frac{1}{u_1^2} - \varsigma^2} \right)^2}} \tag{27}$$

These two results enable to determine equivalently if the constraint is satisfied -or not- for the optimization problem at a fixed frequency, and frequency-by-frequency. From the first result, the result $\mathrm{P}_U(f)$ is compared to $\overline{P}_{\mathrm{r}}$. From the second result, $u_{\mathrm{p}}(f)$ is compared to $u_{\max}(f)$.

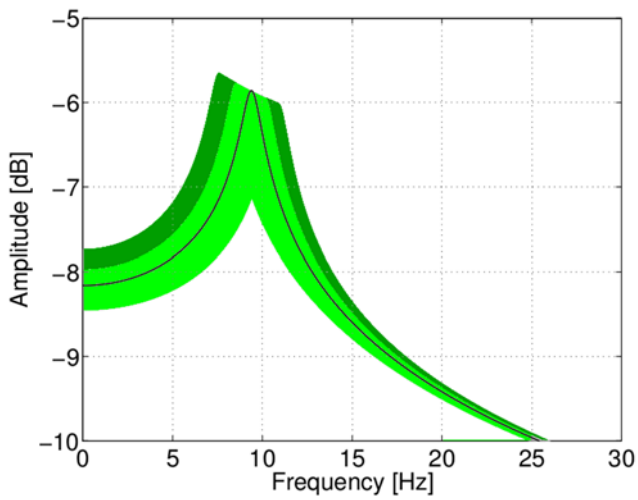

Figure 2: FRF amplitude of a SDOF system having a uniform distribution for the stiffness; the thin line is for the nominal system response; the colored region is for the total amplitude dispersion; the lighted color is for a probability lower than 75%.

To illustrate these results, we chose a SDOF system having a mean of 3500 N and a standard deviation of 700 N. In the Figure 2, the nominal amplitude in function of the frequency is plotted as well as the total dispersion, and the 75% quantile.

6 OPTIMIZATION

To generate the Pareto front, the Normal Boundary Intersection (NBI) method (Das and Dennis 1998) is used to produce a series of constrained single-objective optimizations subproblems. The re-

sulting optimization subproblems are solved by using the Pincus representation formula in conjunction with Nelder-Mead algorithm and the penalty method which deals with the constraints produced by NBI. This leads to the RFNM optimization algorithm (for Representation Formula Nelder-Mead), which permits to find global optima for the Pareto front (Zidani et al. 2013). Explanations about ideas of NBI method and RFNM optimization procedure are given in the appendix section.

For the problem of this work, the NBI first step is to find the solution sets $\mathbf{x}_1^*$ and $\mathbf{x}_2^*$ of both single-objective subproblems, corresponding to the individual global minima of each objectives $\mathcal{F}_1(\mathbf{x}) = \mu_K$ and $\mathcal{F}_2(\mathbf{x}) = -\sigma_K$:

$$\mathbf{x}_1^* = \arg\min_{\mathbf{x}\in\mathcal{S}}\left(\mu_K\right) \tag{28}$$

and:

$$\mathbf{x}_2^* = \arg\min_{\mathbf{x}\in\mathcal{S}}\left(-\sigma_K\right) \tag{29}$$

with the two-parameter vector $\mathbf{x} = \begin{bmatrix} \mu_K \\ \sigma_K \end{bmatrix}$ and where $\mathcal{S}$ is the admissible domain for the design-point solutions (the ones that satisfy all constraints):

$$\mathcal{S}: \begin{cases} \text{Prob}\left[U_K\left(f_j\right) < u_{\max}\left(f_j\right)\right] \geq \overline{P}_{\text{r}}, \quad \text{for } j = 1,\ldots,e \\ \mu_K > \sqrt{3}\sigma_K, \ \sigma_K \geq 0 \\ K \sim \text{Uniform}\left(\mathbf{x}\right). \end{cases} \tag{30}$$

In order to apply the RFNM procedure, each constrained single-objective optimization subproblem formed by the NBI methodology is transformed into non-constrained optimization subproblem by using the penalty methodology (Haftka and Gurdal 1993). Then, by using the Equation (23), problems to solve are:

$$\mathbf{x}_1^* = \min_{\mathbf{x}\in\mathcal{S}_b}\left(\mu_K + \nu\left\|\max\left(\mathbf{0}, \overline{\mathbf{P}}_{\text{r}} - \left(1 - \mathbf{P}_U\left(f\right)\right)\right)\right\|^2\right) \tag{31}$$

and:

$$\mathbf{x}_2^* = \min_{\mathbf{x}\in\mathcal{S}_b}\left(-\sigma_K + \nu\left\|\max\left(\mathbf{0}, \overline{\mathbf{P}}_{\text{r}} - \left(1 - \mathbf{P}_U\left(f\right)\right)\right)\right\|^2\right) \tag{32}$$

for:

$$\mathcal{S}_b : \begin{cases} \mu_K > \sqrt{3}\sigma_K \\ \sigma_K \geq 0 \end{cases} \tag{33}$$

since boundary on the parameters are handled explicitly with the RFNM procedure. In both these expressions, the constant ν is the penalty constant that has to be chosen for our application. This enables to evaluate $f_1^* = \mathcal{F}_1\left(\mathbf{x}_1^*\right)$ and $f_2^* = \mathcal{F}_2\left(\mathbf{x}_2^*\right)$ to form the utopia point $\mathbf{f}^* = \begin{bmatrix} f_1^* & f_2^* \end{bmatrix}^{\mathrm{T}}$.

Next, NBI consists in making a sequential set of $j = \{1, \ldots, l\}$ single objective subproblems, which depends of a parameter $\mathbf{w}_j$ and defined by:

$$\begin{cases} \max\limits_{\mathbf{x}\in\mathcal{S},\, t} t \\ \text{subject to:} \quad \mathbf{\Phi}\mathbf{w}_j + t\mathbf{n} = \mathcal{F}(\mathbf{x}) - \mathbf{f}^*, \end{cases} \tag{34}$$

where $\mathcal{F}(\mathbf{x}) = \begin{bmatrix} \mathcal{F}_1(\mathbf{x}) & \mathcal{F}_2(\mathbf{x}) \end{bmatrix}^{\mathrm{T}} = \begin{bmatrix} \mu_K & -\sigma_K \end{bmatrix}^{\mathrm{T}}$ and:

- $\mathbf{\Phi} = \begin{bmatrix} 0 & \mathcal{F}_1\left(\mathbf{x}_2^*\right) - f_1^* \\ \mathcal{F}_2\left(\mathbf{x}_1^*\right) - f_2^* & 0 \end{bmatrix}$ is the 2×2 pay-off matrix;
- $\mathbf{w}_j$ is a vector of chosen weights for the j-th subproblem and such that $\sum_{i=1}^{2}\left\{\mathbf{w}_j\right\}_i = 1$, $\left\{\mathbf{w}_j\right\}_i \geq 0$; and
- $\mathbf{n}$ is a quasi-normal direction which points towards the point $\mathbf{f}^*$ in the objective space $\mathcal{F}$. It has to be chosen for each application (see the footnote 1 in the next section devoted to the application).

Then, as for the first NBI step, each j constrained single-objective optimization subproblem is transformed into non-constrained optimization subproblem by using the penalty methodology:

$$\min_{\mathbf{x}\in\mathcal{S}_b,\, t}\left(-t + \nu\left\|\mathbf{\Phi}\mathbf{w}_j + t\mathbf{n} - \mathcal{F}(\mathbf{x}) + \mathbf{f}^*\right\|^2 + \nu\left\|\max\left(\mathbf{0}, \overline{\mathbf{P}}_{\mathrm{r}} - \left(1 - \mathbf{P}_U\left(f\right)\right)\right)\right\|^2\right) \tag{35}$$

since boundary on the parameters are handled explicitly with the RFNM procedure.

Next, unconstrained optimization problems given by Equations 31-32 and 35 of NBI method are solved by the RFNM procedure (Zidani et al. 2013). In this procedure, the Pincus representation formula is used to obtain only a set of guess starting points $\mathbf{x}^{(0)}$ for the Nelder-Mead algorithm by generating a small finite sample size of N pseudo-random numbers for the evaluation of the means. This strategy enables to find global optima. Note that it does not use sensitivities, which avoids drawbacks of the involved penalty methodology and makes it efficient.

However, to ensure a better numerical conditioning, objective functions are scaled and replaced throughout the optimization procedure, such that:

$$\mathcal{F}_i \leftarrow a_i\left(\mathcal{F}_i + b_i\right) \tag{36}$$

with a_i and b_i are the application dependent scaling factors.

7 APPLICATION: SDOF WITH A SPECIFIC HULL CONSTRAINT FOR SEVERAL RELIABILITY LEVELS

Points	A	B	C	D	E	F
Frequency [Hz]	0	3	9	12.5	16	29
Amplitude [dB]	-8	-5.5	-5.5	-6.6	-6.6	-10

Table 1: Coordinates of the points that define the amplitude peak response hull for the optimization problems.

This application is defined from the amplitude peak response hull that corresponds to the line segments delimited by points A to F given in the Table 1. The Figure 3 shows the prescribe amplitude peak response hull, as well as a FRF amplitude corresponding to a deterministic SDOF system which belongs to the permissible region, since it is entirely under the curve delimited by the prescribed hull. For this specified hull, several situations were investigated by choosing different values of the admissible reliability levels: $\overline{P}_{\mathrm{r}} = \left\{1,\ 0.93,\ 0.9,\ 0.87,\ 0.83,\ 0.75\right\}$. In addition, we chose to take a unit mass for the numerical application.

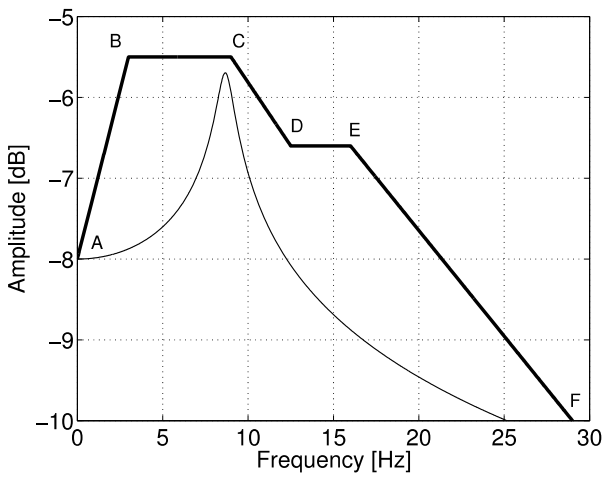

Figure 3: FRF amplitude of one deterministic SDOF system and the available amplitude peak response hull.

In practice, sample size of $N = 70$ pseudo-random numbers are chosen for generating from the Pincus representation formula guess points $\mathbf{x}^{(0)}$ for the Nelder-Mead algorithm (the minimum value seems to be $N = 30$ to obtain meaningful results). Moreover, each optimization from the Nelder-Mead algorithm is repeated by using new samples in order to ensure to find at least 3 times the same minima. From our numerical experience with this application, this procedure ensures to catch the global minimum. For a good resolution, a set of 147 points is chosen to construct the NBI boundary front. For the current application, the scaling factors chosen are $a_1 = 10^{-3}$, $a_2 = 5.10^{-3}$, $b_1 = 0$ and $b_2 = 2.10^3$, and the penalty factor is $\nu = 5.10^4$. Boundary are such that $\mu_K \in \left\{2000, 10000\right\}$ and

$\sigma_K \in \{0,\ 4500\}$. Another parameter to be chosen is the number l of the discretization for the frequency range of interest. The Figure 4 shows the results of investigations for three NBI boundary fronts, having 50, 500 and $5{,}000$ frequency points of discretization, for a reliability level of 100%. We can observe that there is no difference between the last two discretization, demonstrating that a convergence is achieved. To ensure our application results, we take 1,500 points for this discretization in the following.

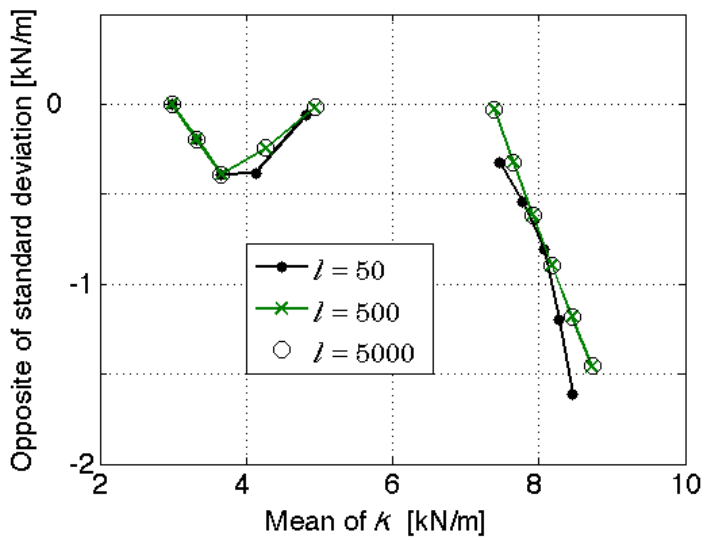

Figure 4: NBI boundary front for several discretization of the frequency range of interest.

Since starting guess points for the Nelder-Mead algorithm comes from samples of random variables, the number of evaluations of the mechanical problem varies for each new run. For a relative stopping criteria of 10^{-4} in the evolution of the objective function or in the evolution of the parameters, it is observed that it is approximately an average of 1,000 evaluations for each point of the NBI front.

Results of the NBI boundary fronts obtained for each admissible reliability level are collected and reported in the Figure 5. Then, the RFNM optimization procedure leads to the six NBI boundary fronts presented in the Figure 5. For a 100% reliability, the front obtained[1] is made of two disjoints parts: the lines segments GH, HL and the line segment IJ. There is no continuity of the front between the point L and the point I since there is no admissible solution for the optimization problem in this

[1] Notice that to obtain this NBI front, the normal $\mathbf{n}$ of the NBI method has to be chosen adequately (we took $\mathbf{n} = \frac{1}{\sqrt{26}}\begin{bmatrix} 5 \\ 1 \end{bmatrix}$ for instance), since only the line segments GH and IJ are obtained with the recommendation of Das and Dennis (1998): $\mathbf{n} = \frac{1}{\sqrt{2}}\begin{bmatrix} 1 \\ 1 \end{bmatrix}$. However, it is not a critical difficulty and the standard choice could be also admissible without any problem since the line segment HL does not holds to the Pareto front (it forms a set of dominated points from the NBI boundary front).

region. To explain the physical meaning of this solution, we can start from the left point G, corresponding to the minimal stiffness that satisfies the optimization constraints. At this design point, the stiffness standard deviation is at its lowest value: it is zero. This is the limit situation where a random system becomes deterministic. So, there is no acceptable uncertainty at this design point. Hence, we consider in this extreme situation that the reliability constraint is respected for any target value. Observing the mechanical system response amplitude helps to better understand the design point G. In fact, the FRF amplitude shown in the Figure 3 is precisely the one of the mechanical system corresponding to this design point G. We can observe in this Figure 3 that the FRF amplitude intersects the available amplitude peak response hull at the null frequency[2]. It is clear from this figure that giving a non-null standard deviation would leads to a dispersion about the nominal response amplitude, which is impossible since there is no margins between the nominal response amplitude and the amplitude peak response hull at this (null) frequency. In addition, one can see that decreasing this optimal meanLfigure-stiffness value would increase the FRF amplitude over all frequencies, hence at the null frequency too, which is also impossible. This explain the meaning of this solution.

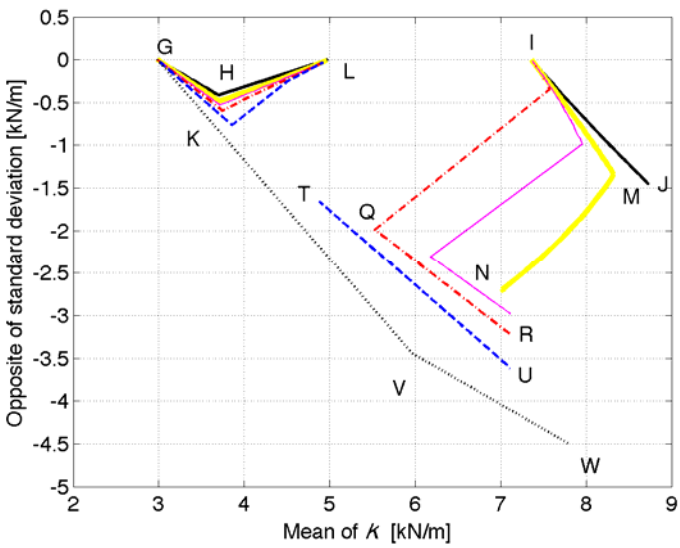

Figure 5: NBI boundary front for several chosen reliabilities: the medium line corresponds to $\overline{P}_r$=100%, the thick line corresponds to $\overline{P}_r$=93%, the thin line corresponds to $\overline{P}_r$=90%, the dash-dot line corresponds to $\overline{P}_r$=87%, the dashed line corresponds to $\overline{P}_r$=83%, the dotted line corresponds to $\overline{P}_r$=75%.

On the contrary, increasing the mean stiffness results in a decrease in the amplitude response of the nominal system at all frequencies, therefore at the null frequency too. This allows the nominal system to go away from the forbidden region delimited by the amplitude peak response hull, enabling now some randomness in the response. Thus, increasing the mean stiffness enables the increase of the stiffness standard deviation, as long as the imposed reliability can be satisfied. So, by increasing the

[2] The null frequency corresponds to a static loading.

mean, the optimal design solutions travels along the NBI front from the design point G to the design point H (Figure 5) for the 100% reliability level. However, we have to keep in mind that increasing the mean stiffness increases also the resonant frequency of the system. Then, the design point H is a limit situation where it becomes impossible to find an admissible solution by increasing the mean stiffness for a same standard deviation. At this design point H, the admissible system response dispersion is simultaneously constrained at two distinct frequencies, namely 0 Hz and 12 Hz, as it is shown in the Figure 6-up-left. Next, it becomes necessary to decrease the standard deviation to enable the stiffness increased, up to the point L. At this design point L, the standard deviation becomes null for a maximal stiffness (see Figure 6-up-right). One can note however that these design solutions, between points H and L, do not belongs to the Pareto front since one objective function is deteriorated when traveling through this way.

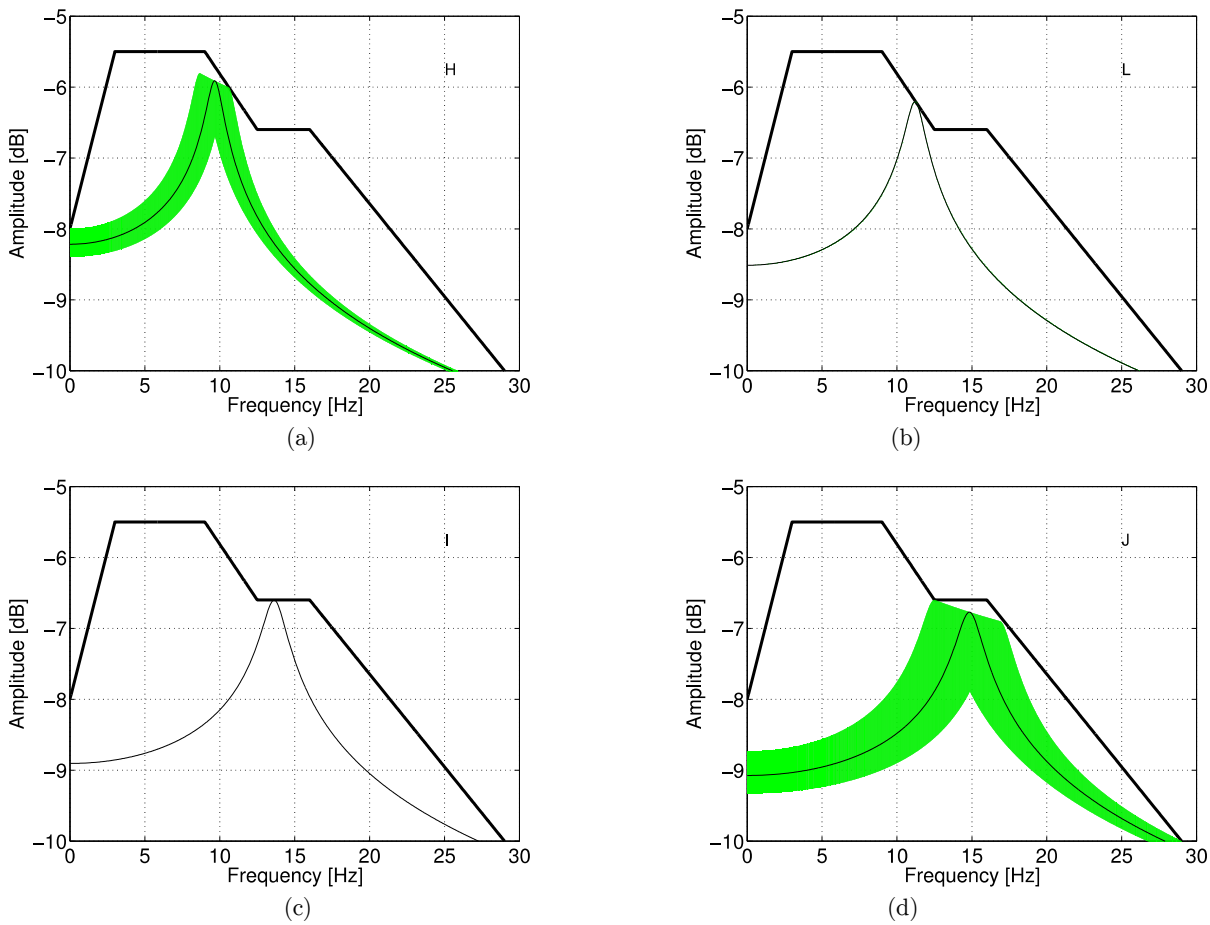

Figure 6: Graphs of the SDOF system FRF amplitude at the design points H (a), L(b), I (c), J (d) for the reliability constraint of 100%; Colored region indicates the total dispersion of the SDOF amplitude, while the thin line indicates the response of the nominal system.

The next admissible point for the 100% reliability is the point I. At this point, the standard deviation is null again, and the stiffness has increased sufficiently to decrease the maximum amplitude

under the constraint hull (see Figure 6-down-left). Then, increasing the stiffness again from this point continued to decrease the amplitude, enabling the possibility of having a non-null, positive, standard deviation. The limit situation becomes now the point J, being the end of the NBI front (see Figure 6-down-right).

Explanations of NBI fronts for the reliability ranging from 93% to 83% are similar. All these fronts share the same left point G and has disjoints parts for the NBI fronts. Differences arise only from the possibility for the SDOF uncertainties to come over the prescribed hull, depending on the required reliability. Frequency response amplitude corresponding to point M and N are presented in Figure 7 for the 93% reliability. One can observe that the point M corresponds to an intersection of the 93% quantile with the constraint hull at 12.5 Hz, while the point N intersects at 4 frequencies, namely 0 Hz, 12.5 Hz, 17 Hz and 29 Hz. Frequency response amplitude corresponding to point Q and R are presented in Figure 8 for the 87% reliability. The point Q corresponds to an intersection of the 87% quantile with the constraint hull at 0 Hz and 12.5 Hz, while the point R intersects at 0 Hz and 29 Hz.

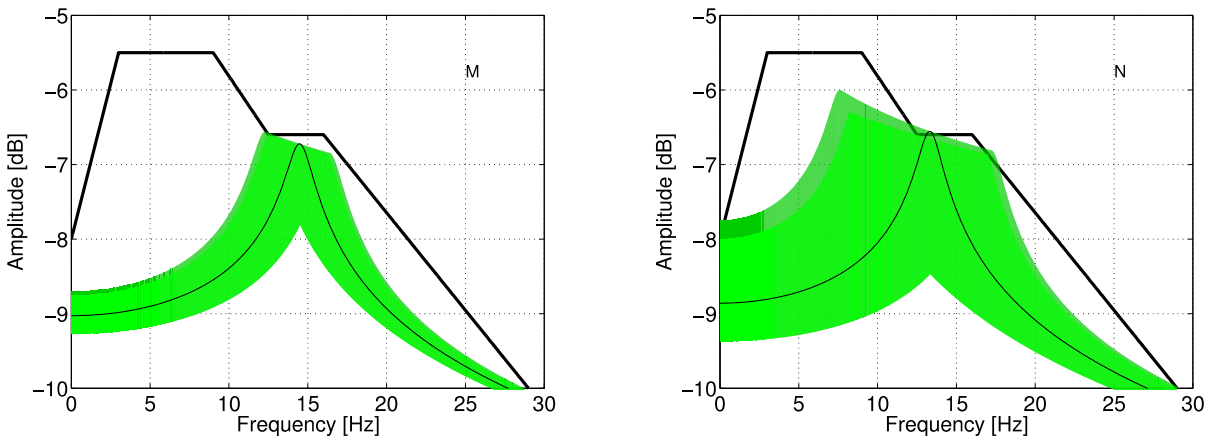

(a) (b)

Figure 7: Graphs of the SDOF system FRF amplitude at the design points M (a) and N (b) for a $\overline{P}_{\mathrm{r}}$=93% reliability. The lighted color region shows the dispersion that respect the reliability constraint (*i.e.* the region corresponding to $\mathrm{P}_U\left(f\right) \leq \overline{P}_{\mathrm{r}}$, the darken color extends this region to show the total dispersion of the SDOF system, while the thin line indicates the response of the nominal system.

For 75% reliability, the front obtained is very simple, with a continuous convex shape between the point G, the point V and the point W. The G point is the same as before. The line segment VW results from the activated constraint: $\mu_K = \sqrt{3}\sigma_K$. Points V and W are illustrated in Figure 9. For the point V, the 75% quantile intersect the constraint hull at the null frequency, while intersection is at 29 Hz for the point W.

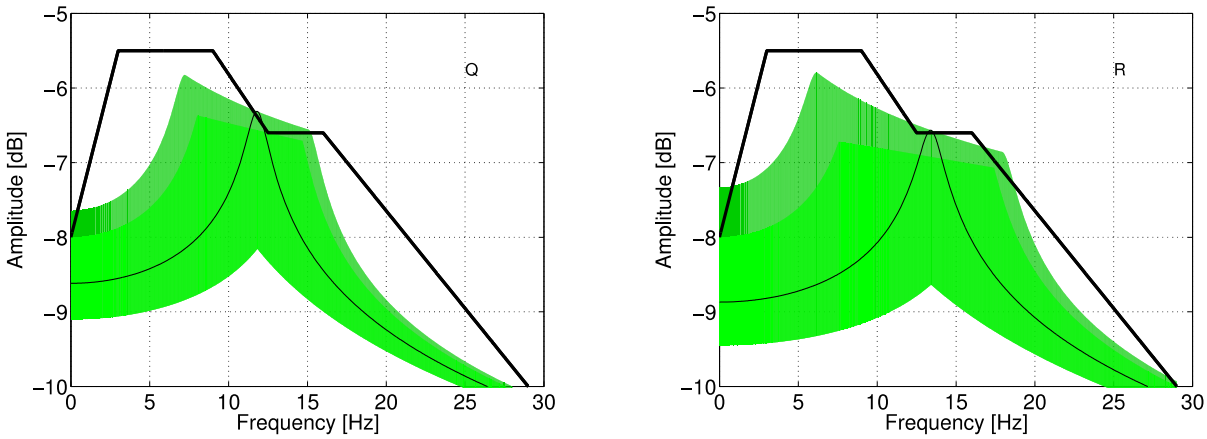

(a) (b)

Figure 8: Graphs of the SDOF system FRF amplitude at the design points Q (a) and R (b) for a $\overline{P}_{\mathrm{r}}$=87% reliability. The lighted color region shows the dispersion that respect the reliability constraint (*i.e.* the region corresponding to $\mathrm{P}_U\left(f\right) \leq \overline{P}_{\mathrm{r}}$, the darken color extends this region to show the total dispersion of the SDOF system, while the thin line indicates the response of the nominal system.

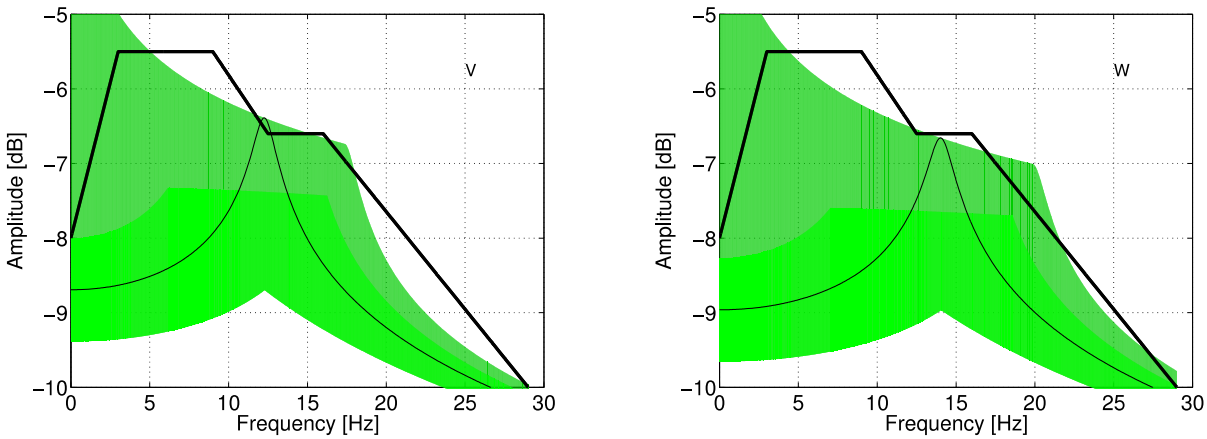

(a) (b)

Figure 9: Graphs of the SDOF system FRF amplitude at the design points V (a) and W (b) for a $\overline{P}_{\mathrm{r}}$=75% reliability. The lighted color region shows the dispersion that respect the reliability constraint (*i.e.* the region corresponding to $\mathrm{P}_U\left(f\right) \leq \overline{P}_{\mathrm{r}}$, the darken color extends this region to show the total dispersion of the SDOF system, while the thin line indicates the response of the nominal system.

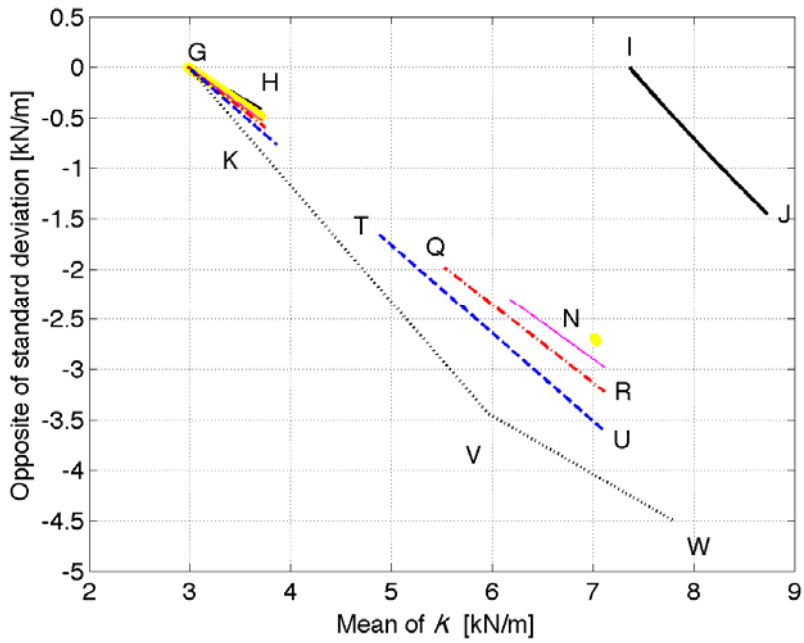

Figure 10: Pareto front for several chosen reliabilities: the medium line corresponds to $\overline{P}_r$=100%, the point corresponds to $\overline{P}_r$=93%, the thin line corresponds to $\overline{P}_r$=90%, the dash-dot line corresponds to $\overline{P}_r$=87%, the dashed line corresponds to $\overline{P}_r$=83%, the dotted line corresponds to $\overline{P}_r$=75%.

Throughout this analysis, it is clear that a filtering is necessary to extract the set of non-dominated points from the NBI boundary front, at the exception of the front of the 75% reliability case. The resulting Pareto front is then constituted from simple disjoints parts, as the Figure 10 illustrates it. The 93% reliability being only a line segment and a single point.

8 CONCLUSIONS

A reliability-based design of a mechanical suspension device is discussed in this study. For the sake of simplification and focusing on the main ideas, it is modeled as a SDOF dynamical system and only the stiffness was considered random. For an assumed bound random variable, the MEP gives the stiffness being a uniform distribution. The main constraint to the problem is the prescription of a peak amplitude hull, where the FRF amplitude of the device has to fit, within the band of frequency of interest. Uncertainty propagation is achieved analytically in this situation. Since the design is reliability based, one must also prescribe the desire reliability $\overline{P}_r$. The greater is this probability, the most strict is the acceptance of the rules.

We choose the mean and the standard deviation of the stiffness as two parameters and two objectives of the optimization problem. The RFNM algorithm is used to solve this reliability-based optimization problem. It is shown that despite the simplicity of the modeling, a SDOF system, an

interesting problem results and, for some choice of the reliability, a not-connected Pareto curve is obtained, meaning that there is a sub-frequency band where there is no solution for the problem.

References

Avriel, M. (1976), Nonlinear programming: Analysis and methods, Englewood Cliffs, NJ.

Bez, E., Souza de Cursi, E., and M.B., G. (2005), A hybrid method for continuous global optimization involving the representation of the solution. In 6th World Congress on Structural and Multidisciplinary Optimization, Rio de Janeiro.

Choi, S., Grandhi, R., and R.A., C. (2007), Reliability-based structural design, Springer.

Das, I. and Dennis, J. (1998), Normal-boundary intersection: a new method for generating pareto optimal point in nonlinear multicriteria optimization problems, SIAM Journal on Optimization, 8:3:631–657.

Haftka, R. and Gurdal, Z. (1993), Elements of structural optimization, Kluwer Academic Publishers, Dordrecht, Netherlands.

Kapur, J. and Kesavan, H. K. (1992), Entropy optimization principles with applications, Academic Press, Inc., London.

Lemaire, M. (2009), Structural reliability, Wiley.

Lin, Y. K. (1967), Probabilistic theory of structural dynamics, McGraw-Hill, Inc., New York.

Luenberger, D. (1973), Introduction to linear and nonlinear programming.

Nelder, J. and Mead, R. (1965), A simplex method for function minimization, Computer Journal, 7:308–313.

Pagnacco, E., Sampaio, R., and Souza de Cursi, E. (2015), Complexity of the response of linear systems with a random coefficient and propagation of uncertainties, Journal of the Brazilian Society of Mechanical Sciences and Engineering, 37:1591–1608. doi: 10.1007/s40430-015-0323-7.

Pincus, M. (1970), A Monte Carlo method for the approximate solution of certain types of constrained optimization problems, Operation Research, 18:1225–1228.

Rubinstein, R. Y. and Kroese, D. P. (2008), Simulation and the Monte Carlo method, John Wiley & Sons, Inc., New Jersey, USA.

Souza de Cursi, E. (2007), Representation of solutions in variational calculus, E. Tarocco; E. A. de Souza Neto; A. A. Novotny , (Org.). Variational Formulations in Mechanics: Theory and Applications. Barcelona , (CIMNE).

Souza de Cursi, E. and Sampaio, R. (2015), Uncertainty quantification and stochastic modeling with matlab, Elsevier, ISTE Press.

Souza de Cursi, E., Bez, E., and Goncalves, M. (2008), A procedure of global optimization and its application to estimate parameters in interaction spatial models. In EngOpt 2008.

Zidani, H., Pagnacco, E., Sampaio, R., Ellaia, R. and Souza de Cursi, E. (2013), Multi-objective optimization by a new hybridized method: applications to random mechanical systems, Engineering Optimization, 45:8: 917–939. doi: 10.1080/0305215X.2012.713355.

Zwillinger, D. and Kokoska, S. (2000), Standard probability and statistics tables and formulae, Chapman & Hall/CRC, New York, USA.

A Procedure to Solve the Multi-Objective Optimization Problem

This work uses the Normal Boundary Intersection (NBI) method of Das and Dennis (1998) in conjunction with the RFNM procedure (Zidani et al. 2013) to find the Pareto front of the multi-objective optimization problem. The NBI method leads to a sequence of constrained single-objective problems. Then, these problems are transformed into unconstrained problems through a penalty method in

order to be solved by the RFNM procedure. Optimum solutions of this sequence enable to construct a pointwise approximation of the efficient Pareto front.

A.1 NBI method

Multi-objective optimization involves the simultaneous optimization of n incommensurable, and often competing, objectives $\mathcal{F}_i(\mathbf{x})$:

$$\min_{\mathbf{x}\in\mathcal{S}} \quad \mathcal{F}(\mathbf{x}) = \left[\begin{array}{ccc} \mathcal{F}_1(\mathbf{x}) & \dots & \mathcal{F}_q(\mathbf{x}) \end{array} \right]^{\mathrm{T}} \tag{37}$$

for parameters $\mathbf{x}\in\mathcal{S}$. In the absence of any preference information, a non-dominated set of solutions, termed as Pareto optimal solutions, is sought. This is illustrated in Figure 11 for the minimization of a two-objective function. The most popular method to solve this problem is the weighted sum approach (Haftka and Gurdal 1993). But this method has the major drawback of not being able to generate an extended set of optimal Pareto solutions even for a uniform distribution of the weighting coefficients. In response to the failure of the weighted sum method, Das and Dennis (1998) have proposed the NBI method, which can produce a collection of even spread points on the Pareto front. NBI works by transforming the multi-objective optimization problem into a set of nonlinear programming subproblems from a geometrically intuitive parameterization. This strategy produces a set of points on the Pareto front, giving an accurate picture of the whole front. This strategy can be considered as the state-of-the-art regarding deterministic methods.

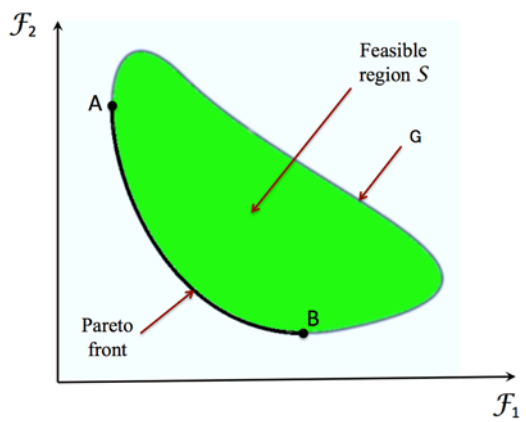

Figure 11: Pareto front for the minimization of two-objective function.

In order to explain the idea of the NBI method, let us define:

- $\mathbf{x}_i^*$ the solution vector for the individual function $\mathcal{F}_i(\mathbf{x})$ of the optimization problem in the feasible region, $i = 1,...,q$.
- $\mathbf{f}(\mathbf{x}_i^*) = \left[\begin{array}{ccc} \mathcal{F}_1(\mathbf{x}_i^*) & \dots & \mathcal{F}_q(\mathbf{x}_i^*) \end{array} \right]^{\mathrm{T}}$ the vector of the objective functions evaluated at the solution $\mathbf{x}_i^*$.

- $\mathbf{f}^* = \left[\begin{array}{ccc} \mathcal{F}_1(\mathbf{x}_1^*) & \ldots & \mathcal{F}_q(\mathbf{x}_q^*) \end{array} \right]^{\mathrm{T}}$ the vector of the individual optimal solutions for the objective functions (*i.e.*, the utopia point or shadow minimum).
- $\mathbf{\Phi}$ the $q \times q$ pay-off matrix in which the i-th column is $\mathbf{f}(\mathbf{x}_i^*) - \mathbf{f}^*$:

$$\mathbf{\Phi} = \begin{pmatrix} 0 & f_1(x_2^*) - f_1(x_1^*) & \cdot & \cdot & \cdot & f_1(x_q^*) - f_1(x_1^*) \\ f_2(x_1^*) - f_2(x_2^*) & 0 & \cdot & \cdot & \cdot & f_2(x_q^*) - f_2(x_2^*) \\ \cdot & & & & & \cdot \\ \cdot & & & \cdot & & \cdot \\ \cdot & & & & \cdot & \cdot \\ f_q(x_1^*) - f_q(x_q^*) & & \cdot & \cdot & \cdot & 0 \end{pmatrix} \tag{38}$$

In these conditions, the set of the point of $\mathbb{R}^q$, convex combination of $\mathbf{f}(\mathbf{x}_i^*) - \mathbf{f}^*$, *i.e.* $\left\{ \mathbf{\Phi w} \colon \mathbf{w} \in \mathbb{R}^q,\ \sum_{i=1}^{q} \mathbf{w}_i = 1;\ \mathbf{w}_i \geq 0 \right\}$, is the so-called Convex Hull Individual Minima (CHIM). This is illustrated in Figure 12(a) for the minimization problem presented in the Figure 11.

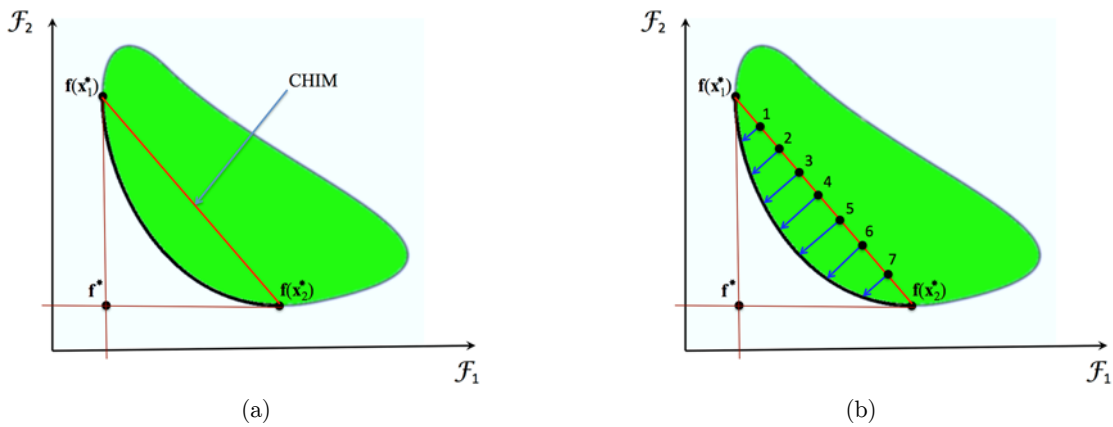

Figure 12: (a) CHIM representation for a minimization problem of two-objective function; and (b) 7 NBI subproblems to solve.

The purpose of NBI is to find the portion of space that contains the Pareto optimal front. In the Figure 11, this front is reduced to the black curve between the points A (*i.e.* $\mathbf{f}\left(\mathbf{x}_1^*\right)$) and B (*i.e.* $\mathbf{f}\left(\mathbf{x}_2^*\right)$) near the axes origin. The algebraic idea behind this approach is simple and evident: the intersection between the border Γ and the normal pointing toward the origin from any point of the CHIM is a point of the portion of Γ which contains the Pareto optimal points. That is to look for the maximum distance between a point of CHIM and Γ border by pointing to the origin. This is illustrated in Figure 12(b) for the minimization problem presented by the Figure 11. For a barycentric coordinate $\mathbf{w}$, $\mathbf{\Phi w}$ represents a point of CHIM. They are black points, numbered from 1 to 7 in

Figure 12(b). Let us denote by $\mathbf{n}$ the unit normal vector to the CHIM pointing to the origin. Under these conditions $\mathbf{\Phi w} + t\mathbf{n},\ t \in \mathbb{R}$, represents the set of points on this normal. The intersection of the normal $\mathbf{n}$ and Γ boundary closest to the origin is the global solution of the following problem:

$$\begin{cases} \max\limits_{\mathbf{x}\in\mathcal{S},t} \ t \\ \text{subject to:} \quad \mathbf{\Phi w} + t\mathbf{n} = \mathcal{F}(\mathbf{x}), \end{cases} \tag{39}$$

Note that if the origin is not taken in $\mathbf{f}^*$, the constraint should be written in the form $\mathbf{\Phi w} + t\mathbf{n} = \mathcal{F}(\mathbf{x}) - \mathbf{f}^*$. We obtain a new formulation denoted NBI($\mathbf{w}$) for the minimization problem:

$$\text{NBI}(\mathbf{w}): \begin{cases} \max\limits_{\mathbf{x}\in\mathcal{S},t} \ t \\ \text{subject to:} \quad \mathbf{\Phi w} + t\mathbf{n} = \mathcal{F}(\mathbf{x}) - \mathbf{f}^*, \end{cases} \tag{40}$$

The idea is to solve NBI($\mathbf{w}$) for different values of $\mathbf{w}$ and find different points of the Γ limit and thus effectively build an approximation of the efficient front. In Figure 12(b), 7 blue arrows, producing 7 points of the Pareto front, illustrates this.

Generally, the vector $\mathbf{n}$ can be chosen almost normal with negative components (points to the origin), and the results will be the same. For general situations, it is a quasi-normal direction as a linear combination of $\mathbf{\Phi}$ columns, multiplied by -1 to provide a direction toward the origin:

$$\mathbf{n} = -\frac{\mathbf{\Phi 1}_q}{\left\|\mathbf{\Phi 1}_q\right\|} \tag{41}$$

where $\mathbf{1}_q$ is the all-ones column vector.

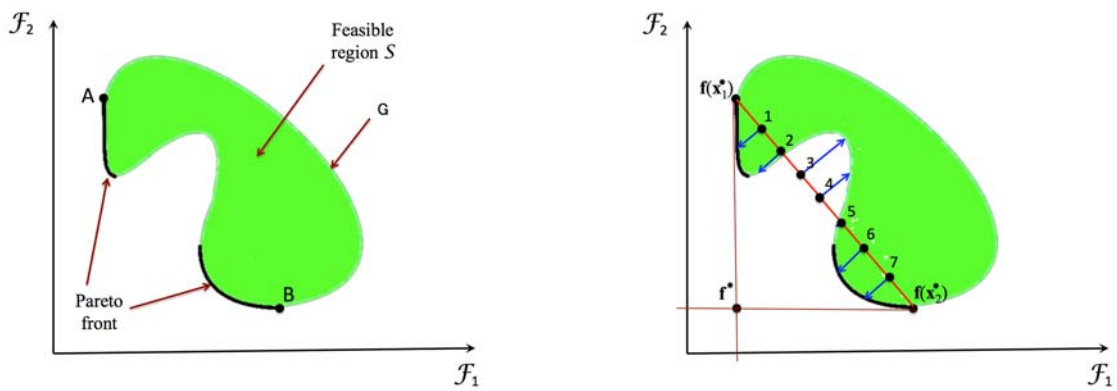

Figure 13: (a) Pareto front for a specific problem of minimization of two-objective function having a non-convex feasible region; and (b) illustration of NBI subproblems generated from a 7 points discretization of the CHIM obtained for this problem.

But the points thus obtained are not necessarily Pareto optimal points. To illustrate this assertion, the Figure 13 shows the Pareto front and solutions obtained from seven points of CHIM for a specific minimization problem with two-objective function having a non-convex feasible region. In this figure, it is clear that the points numbered 2 to 5 are not Pareto optimal, although they were found by the NBI method. As a consequence, a filtering procedure must be involved in post-processing, once NBI subproblems solutions are produced, in order to obtain the Pareto front.

A.2 Solving NBI subproblems by the RFNM procedure

The set of nonlinear programming subproblem obtained from the NBI method are solved by the RFNM procedure (Zidani et al. 2013). RFNM procedure is a hybrid Nelder-Mead simplex search with integral representation formula of Pincus and genetic algorithm. But it is a procedure to solve an unconstraint optimization problem. Then, constrained sub-problems obtained from the NBI method are first transformed into unconstrained sub-problems by using the penalty method (Luenberger 1973, Avriel 1976, Haftka and Gurdal 1993).

For solving optimization problems, Nelder and Mead (1965) algorithm is well known for its ease of use. It is a simple direct search technique that does not need to take derivatives of the function under exploration. One interesting feature of this algorithm is its ability to handle difficult objective functions such as the one obtained here by using the penalty method. However, it is a local approach. As a consequence, it is very sensitive to the choice of initial points and does not ensure to attain the global optimum. Hence, it is interesting to hybridize it with the formula method of Pincus (1970) and genetic algorithm to generate the initial point.

In the literature, representation formulae have been introduced in order to characterize explicitly solutions to the generic problem:

$$\mathbf{x}^* = \arg\min_{\mathbf{x}\in\mathcal{S}} \mathcal{L}(\mathbf{x}) \tag{42}$$

where it is assumed that many minima may exist on $\mathcal{S}$ from which there is a single optimal point $\mathbf{x}^*$. For instance, Pincus (1970) has proposed the representation formula:

$$\mathbf{x}^* = \lim_{\varrho\to+\infty} \frac{\int_S \mathbf{x}\ \mathrm{e}^{-\varrho\mathcal{L}(x)}\mathrm{d}\mathbf{x}}{\int_S \mathrm{e}^{-\varrho\mathcal{L}(x)}\mathrm{d}\mathbf{x}} \tag{43}$$

More recently, this representation has been reformulated by Souza de Cursi (2007) as follows: let $\mathbf{X}$ be a random variable taking its values on $\mathcal{S}$ and $\delta:\mathbb{R}^2\to\mathbb{R}$ be a function. If these elements are conveniently chosen, then:

$$\mathbf{x}^* = \lim_{\lambda\to+\infty} \frac{\mathrm{E}\left[\mathbf{X}\ \delta\left(\lambda,\mathcal{L}(\mathbf{X})\right)\right]}{\mathrm{E}\left[\delta\left(\lambda,\mathcal{L}(\mathbf{X})\right)\right]} \tag{44}$$

where $\mathrm{E}\left[\bullet\right]$ denotes the expectation operator. It is a weighted mean of the points $\mathbf{x}\in\mathcal{S}$, where the weight decreases when $\mathcal{L}(\mathbf{X})$ increases. The term $\delta\left(\lambda,\mathcal{L}(\mathbf{X})\right)$ in the representation formula vanishes

for points having values higher than $\mathcal{L}(\mathbf{x}^*)$ when $\lambda \to +\infty$. The formulation of Pincus corresponds to $\delta\left(\lambda,s\right) = \mathrm{e}^{-\lambda s}$ and this is a convenient choice. The general properties of $\mathbf{X}$ and δ are detailed in Bez et al. (2005) and Souza de Cursi et al. (2008) but $\mathbf{X}$ uniformly distributed is a convenient choice.

In practice, the numerical implementation uses a large value of λ. A finite sample of $\mathbf{X}$ is generated, according to the chosen probability distribution. This consists in generating N admissible points $(\mathbf{x}_1,\mathbf{x}_2,...,\mathbf{x}_N) \in \mathcal{S}$. In addition, empirical means are used:

$$\mathbf{x}^* \simeq \frac{\sum_{i=1}^{N} \mathbf{x}_i \ \delta\left(\lambda,\mathcal{L}(\mathbf{x}_i)\right)}{\sum_{i=1}^{N} \delta\left(\lambda,\mathcal{L}(\mathbf{x}_i)\right)} \tag{45}$$

The method obtained by hybridization of Nelder-Mead with the representation formula of Pincus and the genetic algorithm to generate the initial point is called RFNM (Zidani et al. 2013). It is an improvement of the Nelder-Mead algorithm by using the representation formula to find the region containing the global solution, based on the generation of finite samples of the random variables involved in the expression and an approximation of the limits.